

Mass Spectra from Turbulent Fragmentation

Ralf S. Klessen^{1,2}

¹ UCO/Lick Observatory, University of California at Santa Cruz, Santa Cruz, CA 95064, USA

² Max-Planck-Institut für Astronomie, Königstuhl 17, 69117 Heidelberg, Germany

Abstract. Turbulent fragmentation determines where and when protostellar cores form, and how they contract and grow in mass from the surrounding cloud material. This process is investigated, using numerical models of molecular cloud dynamics. Molecular cloud regions without turbulent driving sources, or where turbulence is driven on large scales, exhibit rapid and efficient star formation in a clustered mode, whereas interstellar turbulence that carries most energy on small scales results in isolated star formation with low efficiency. The clump mass spectrum of shock-generated density fluctuations in pure hydrodynamic, supersonic turbulence is not well fit by a power law, and it is too steep at the high-mass end to be in agreement with the observational data. When gravity is included in the turbulence models, local collapse occurs, and the spectrum extends towards larger masses as clumps merge together, a power-law description $dN/dM \propto M^\nu$ becomes possible with slope $\nu \lesssim -2$. In the case of pure gravitational contraction, i.e. in regions without turbulent support, the clump mass spectrum is shallower with $\nu \approx -3/2$. The mass spectrum of protostellar cores in regions without turbulent support and where turbulence is replenished on large-scales, however, is well described by a log-normal or by multiple power laws, similar to the stellar IMF at low and intermediate masses. In the case of small-scale turbulence, the core mass spectrum is too flat compared to the IMF for all masses.

1 Introduction

Stars are born in turbulent interstellar clouds of molecular hydrogen. The location and the mass growth of young stars are hereby intimately coupled to the dynamical cloud environment. Stars form by gravitational collapse of shock-compressed density fluctuations generated from the supersonic turbulence ubiquitously observed in molecular clouds (e.g. Elmegreen 1993, Padoan 1995, Klessen, Heitsch, & Mac Low 2000). Once a gas clump becomes gravitationally unstable, it begins to collapse and the central density increases considerably, giving birth to a protostar. As stars typically form in small aggregates or larger clusters (Lada 1992, Adams & Myers 2001) the interaction of protostellar cores and their competition for mass growth from their surroundings are important processes determining the distribution of stellar masses. These complex phenomena are addressed by analyzing and comparing numerical models of self-gravitating supersonic turbulence. Focus is on the connection between supersonic turbulence and local collapse and on the relation between the mass spectra of transient gas clumps and protostellar cores.

2 Numerical Models of Turbulent Molecular Clouds

To adequately describe turbulent fragmentation and the formation of protostellar cores, it is necessary to resolve the collapse of shock compressed regions over several orders of magnitude in density. To achieve this, I use SPH (*smoothed particle hydrodynamics*) which is a well-known particle-based Lagrangian method to solve the equations of hydrodynamics. Details about the numerical implementation can be found in Klessen & Burkert (2000).

In the current paper I consider different scenarios for interstellar turbulence. Model 1 completely lacks turbulent support (it describes the contraction of Gaussian density distribution, Klessen & Burkert 2000, 2001), model 2 describes freely decaying supersonic turbulence, and in models 3 to 5 turbulence is continuously driven. The non-local driving scheme inserts kinetic energy in a specified range of wavenumbers, $1 \leq k \leq 2$, $3 \leq k \leq 4$, and $7 \leq k \leq 8$, corresponding to sources that act on large, intermediate, and small scales, respectively (Mac Low 1999, Klessen et al. 2000), such that an rms Mach number of $\mathcal{M}_{\text{rms}} = 5.5$ is maintained throughout the evolution.

3 Star Formation from Turbulent Fragmentation

Stars form from turbulent fragmentation of molecular cloud material. Supersonic turbulence, even if strong enough to counterbalance gravity on global scales, will usually *provoke* local collapse. Turbulence establishes a complex network of interacting shocks, where converging shock fronts generate clumps of high density. This density enhancement can be large enough for the fluctuations to become gravitationally unstable and collapse. However, the fluctuations in turbulent velocity fields are highly transient and the same random flow that creates local density enhancements can disperse them again. For local collapse to actually result in the formation of stars, Jeans-unstable shock-generated density fluctuations must collapse to sufficiently high densities on time scales shorter than the typical time interval between two successive shock passages. The shorter the time between shock passages, the less likely these fluctuations are to survive. Hence, the timescale and efficiency of protostellar core formation depend strongly on the wavelength and strength of the driving source (Klessen et al. 2000, Heitsch et al. 2001), and accretion histories of individual protostars are strongly time varying (Klessen 2001).

The velocity field of long-wavelength turbulence is dominated by large-scale shocks which are very efficient in sweeping up molecular cloud material, thus creating massive coherent density structures. When a coherent region reaches the critical density for gravitational collapse its mass typically exceeds the local Jeans limit by far. Inside the shock compressed region, the velocity dispersion is much smaller than in the ambient turbulent flow and the situation is similar to localized turbulent decay. Quickly a cluster of protostellar cores forms. Therefore, models 1 to 3 lead to a *clustered* mode of star formation. The efficiency of turbulent fragmentation is reduced if the driving wavelength decreases. When

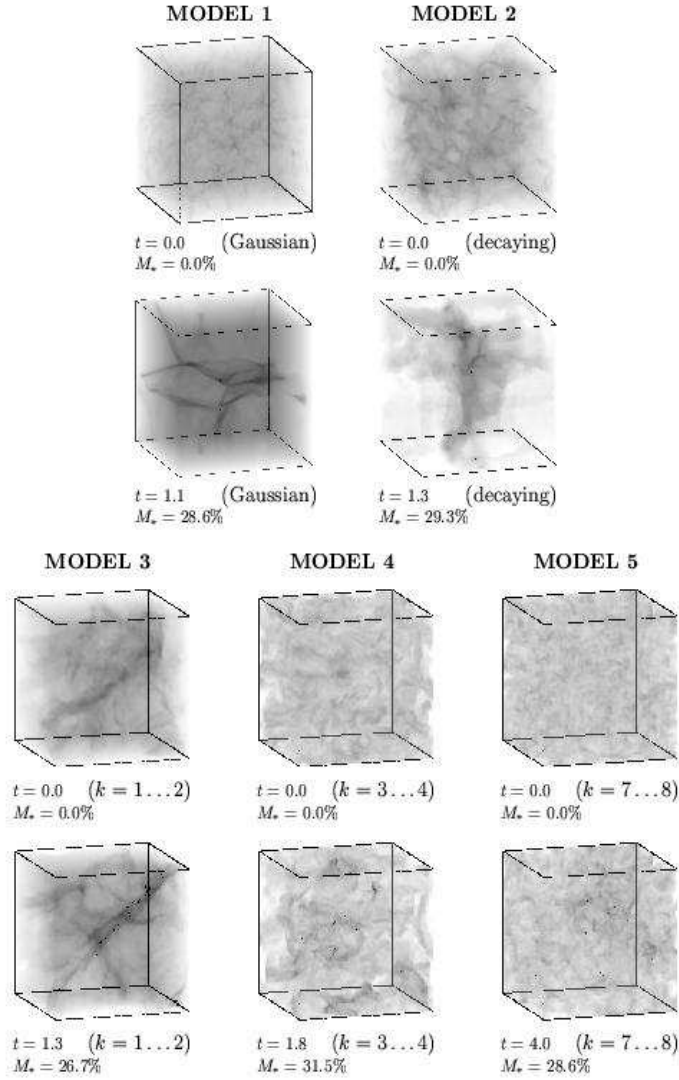


Fig. 1. Comparison of the gas distribution in the five models at two different phases of the dynamical evolution, at $t = 0$ indicating the initial density structure, just before gravity is ‘switched on’, and after the first cores have formed and accumulated roughly $M_* \approx 30\%$ of the total mass. The high-density (protostellar) cores are indicated by black dots. Note the different time interval needed to reach the same dynamical stage. Time is normalized to the global free-fall timescale of the system, which is $\tau_{\text{ff}} = 10^5$ yr for $T = 11.4$ K and $n(\text{H}_2) = 10^5 \text{ cm}^{-3}$. The cubes contain masses of $220 \langle M_J \rangle$ (models 1 and 2) and $120 \langle M_J \rangle$ (models 3 to 5), respectively, where the average thermal Jeans mass is $\langle M_J \rangle = 1 M_\odot$ with the above scaling. The considered volumes are $(0.32 \text{ pc})^3$ and $(0.29 \text{ pc})^3$, respectively.

energy is inserted mainly on small spatial scales, the network of interacting shocks is very tightly knit, and protostellar cores form independently of each other at random locations throughout the cloud and at random times. Individual shock generated clumps have lower mass and the time interval between two shock passages through the same point in space is small. Hence, collapsing cores are easily destroyed again and star formation is inefficient. This scenario corresponds to the *isolated* mode of star formation.

This is visualized in Figure 1, showing the density structure of all five models initially and at a time when the first protostellar cores have formed by turbulent fragmentation and have accreted roughly 30% of the total mass. Note the different time interval needed to reach this dynamical state and the large variations in the resulting density distribution between the various models. Dark dots indicate the location of dense collapsed cores.

4 Mass Spectra from Turbulent Fragmentation

To illustrate the relation between the masses of molecular clumps, protostellar cores and the resulting stars, Figure 2 plots for the five models the mass distribution of all gas clumps, of the subset of Jeans-critical clumps, and of collapsed cores at four different evolutionary stages – clumps are defined as described in Appendix 1 of Klessen & Burkert (2000).

In the initial, completely pre-stellar phase the clump mass spectrum is not well described by a single power law. The distribution has small width and falls off steeply at large masses. Below masses $M \approx 0.3 \langle M_J \rangle$ the distribution becomes shallower, and strongly declines at and beyond the resolution limit (indicated by a vertical line). Clumps are on average considerably smaller than the mean Jeans mass in the system $\langle M_J \rangle$.

Gravity strongly modifies the distribution of clump masses during the later evolution. As gas clumps merge and grow bigger, their mass spectrum becomes flatter and extends towards larger masses. Consequently, the number of clumps that exceed the Jeans limit grows, and local collapse sets in leading to the formation of dense condensations. This is most evident in models 1 and 2 where the velocity field is entirely determined by gravitational contraction on all scales. The clump mass spectrum in intermediate phases of the evolution (i.e. when protostellar cores are forming, but the overall gravitational potential is still dominated by non-accreted gas) exhibits a slope -1.5 similar to the observed one. When the velocity field is dominated by strong (driven) turbulence, the effect of gravity on the clump mass spectrum is much weaker. It remains steep, close to or even below the Salpeter value. This is most clearly seen for small-wavelength turbulence. Here, the short interval between shock passages prohibits efficient merging and the build up of a large number of massive clumps. Only few fluctuations become Jeans unstable and collapse to form protostars. These form independent of each other at random locations and times and typically do not interact. Increasing the driving wavelength leads to more coherent and rapid star formation.

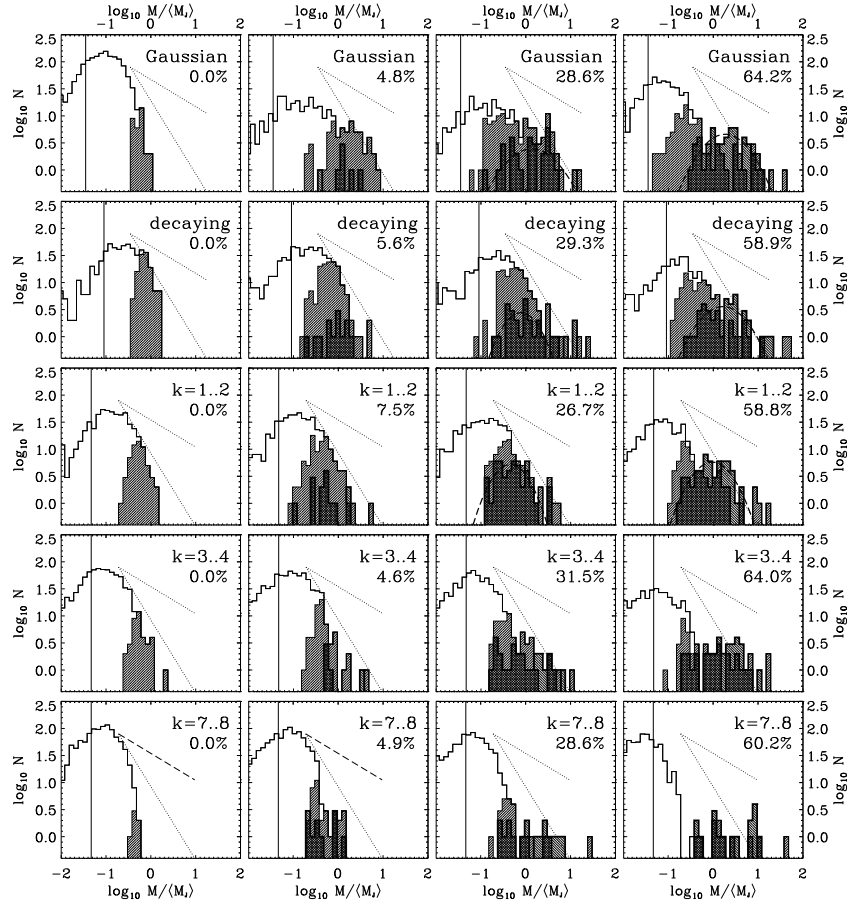


Fig. 2. Mass spectra of gas clumps (thin lines), and of the subset of Jeans unstable clumps (thin lines, hatched distribution), and of dense collapsed cores (hatched thick-lined histograms). Masses are binned logarithmically and normalized to the average thermal Jeans mass $\langle M_J \rangle$. The left column gives the initial state of the system, just when gravity is ‘switched on’, the second column shows the mass spectra when $M_* \approx 5\%$ of the mass is accreted onto dense cores, the third column describes $M_* \approx 30\%$, and the last one $M_* \approx 60\%$. For comparison with power-law spectra ($dN/dM \propto M^\nu$), a slope $\nu = -1.5$ typical for the observed clump mass distribution, and the Salpeter slope $\nu = -2.33$ for the IMF at intermediate and large masses, are indicated by the dotted lines in each plot. Note that with the adopted logarithmic mass binning these slopes appear shallower by +1 in the plot. The vertical line shows the SPH resolution limit. In columns 3 and 4, the long dashed curve shows the best log-normal fit to the core mass spectrum. To compare the distribution of core masses with the stellar IMF, an efficiency factor of roughly 1/3 to 1/2 for the conversion of protostellar core material into single stars needs to be taken into account. For $T = 11.4 \text{ K}$ and $n(\text{H}_2) = 10^5 \text{ cm}^{-3}$, the average Jeans mass in the system is $\langle M_J \rangle = 1 M_\odot$.

Long-wavelength turbulence or turbulent decay leads to a core mass spectrum that is well approximated by a *log-normal*. It roughly peaks at the *average thermal Jeans mass* $\langle M_J \rangle$ of the system and is comparable in width with the observed IMF (Klessen & Burkert 2000, 2001). The log-normal shape of the mass distribution may be explained by invoking the central limit theorem (e.g. Zinnecker 1984), as protostellar cores form and evolve through a sequence of highly stochastic events (resulting from supersonic turbulence and/or competitive accretion). To find the mass peak at $\langle M_J \rangle$ may be somewhat surprising given the fact that the local Jeans mass strongly varies between different clumps. In a statistical sense the system retains knowledge of its mean properties. The total width of the core distribution is about two orders of magnitude in mass and is approximately the same for all four models. However, the spectrum for intermediate and short-wavelength turbulence, i.e. for isolated core formation, is too flat (or equivalently too wide) to be comparable to the observed IMF. This is in agreement with the hypothesis that most stars form in aggregates or clusters.

The current findings raise considerable doubts about attempts to explain the stellar IMF from the turbulence-induced clump mass spectrum *only* (e.g. Elmegreen 1993, Padoan 1995, Padoan & Nordlund 2001). Quite typically for star forming turbulence, the collapse timescale of shock-compressed gas clumps often is comparable to their lifetime (molecular cloud clumps appear to be very transient, e.g. Bergin et al. 1997). While collapsing to form or feed protostars, clumps may lose or gain matter from interaction with the ambient turbulent flow. In a dense cluster environment, collapsing clumps may merge to form larger clumps containing multiple protostellar cores, which subsequently compete with each other for accretion from the common gas environment. As consequence, the resulting distribution of clump masses in star forming regions strongly evolves in time (Figure 2). It is not possible to infer a *one-to-one* relation between the clump masses resulting from turbulent molecular cloud fragmentation and the stellar IMF. It is not appropriate to take a snapshot of the turbulent clump mass spectrum as describing the IMF.

References

1. Adams, F. C., Myers, P. C. 2001, ApJ, in press (astro-ph/0102039)
2. Bergin, E. A., Goldsmith, P. F., Snell, R. L., Langer, W. D. 1997, ApJ, 428, 285
3. Elmegreen, B. G. 1993, ApJ, 419, L29
4. Heitsch, F., Mac Low, M.-M., Klessen, R. S. 2001, ApJ, 547, 280
5. Klessen, R. S. 2001, ApJ, 550, L77
6. Klessen, R. S., Burkert, A. 2000, ApJS, 128, 287
7. Klessen, R. S., Burkert, A. 2001, ApJ, 549, 386
8. Klessen, R. S., Heitsch, F., Mac Low, M.-M. 2000, ApJ, 535, 887
9. Lada, E., 1992, ApJ, 393, L25
10. Mac Low, M.-M., 1999, ApJ, 524, 169
11. Mac Low, M.-M., Klessen, R. S., Burkert, A., Smith, M. D. 1998, PRL, 80, 2754
12. Padoan, P. 1995, MNRAS, 277, 337
13. Padoan, P., Nordlund, Å. 2001, ApJ, submitted (astro-ph/0011465)
14. Zinnecker, H. 1984, MNRAS, 210, 43